

Effect of floor slabs on the seismic performance of RC frames

S.M Ahmed & U. Gunasekaran

Anna University, Chennai, India.



2014 NZSEE
Conference

ABSTRACT: In monolithic reinforced concrete structures, portions of the floor slabs act as flanges to the girders, thereby increasing the strength and stiffness of the girders. The question of how much the slab contributes to the lateral strength is very important for the design of structures; therefore this paper describes the effect of slabs at the joints in moment-frame structures subjected to large seismic deformations. A simple method to model a beam-column joint subassembly including the effects of both beam growth/elongation and the floor slab is introduced. The model is developed by establishing the slab crack pattern at the joint and the state of strain in the slab bars. The results of the models excluding and including slab effects are verified with the experiential test results. The joint model is incorporated in the nonlinear dynamic analyses for a five-storey and four-bay moment frame structure. Two different ground motions (El-Centro 1940 and Northridge 1994) are considered for the analyses. The results show that the cyclic inelastic bending causes the beams to increase in length and the floor slabs significantly restrain this phenomenon and cause the columns to displace by different amounts, changing the distribution of shear among the columns, and increasing the base shear of the columns. These additional forces may lead to a failure mechanism different from the anticipated one. The effect of floor slab including beam elongation effect is thus illustrated for a two dimensional moment frame building and this model works well for the lateral load analysis of frames.

1 INTRODUCTION

The behaviour of RC beam-column connections are complex and several experimental investigations have been conducted in the last three decades to identify the failure initiation mechanism, to make the necessary design changes to prevent a catastrophic failure. However, the floor slabs effect were underestimated or ignored for the seismic performance of buildings. In seismic conditions involving reversed cyclic loading, anchorage requirements assume great importance in deciding the sizes of the members, also the requirement of adequate flexural strength of columns, to ensure beam yield mechanism. The case of the bond deterioration for the beam bars which passing through the joint region will prevent the beam flexural yielding and allows the yielding to be extended to the column, this type of detailing is referred as “gravity load frame” (non-seismic frame) and this might cause severe strength degradation leading to particularly brittle failure mechanism.

Formation of the plastic hinges at the beam ends near the column face will produce the beam elongation phenomena, due to concrete cracking and yielding of the main reinforcement under revised cyclic loading. This phenomenon (“beam elongation”) was first described by Fenwick and Fong (1979); and it was very clearly seen in the 2010-2011 Canterbury earthquakes.

Several analytical techniques were conducted to investigate the behaviour of beam-to-column joints subjected to cyclic loading. These studies utilized both bond-slip deformations and joint shear deformation in poorly detailed RC frame joints, e.g. Filippou (1993); Elmorsi et al (2000); Calvi et al (2002); Fabbrocino et al (2004); Eligehausen et al (2006); and Favvata et al (2008). Most of these researches concluded that the strength loss in joints cannot be predicted accurately by considering bond-slip response and employing a slip-based failure criterion. Despite the extensive analytical and

experimental studies conducted, discrepancy still exists between these studies in accurately predicting the shear capacity of the joints. The errors were mainly due to elongation of plastic hinges not being captured accurately. However, in all these models floor slab has been neglected or only partially considered (Unal and Burak 2013) as a strength contributing factor for seismic performance of the joints. Also these models did not account together for the beam elongation and slab effects at the connections. Fenwick and Davidson (1995) proposed a simple analytical model for beam elongation without considering the slab effect. A six storey, three-bay frame was analyzed, with and without the beam elongation elements. The greater beam elongation occurred with greater beam depths and storey drift ratios; so they have suggested that the beam elongation is proportional to the beam depth h_b and to the number of bays n_b . A beam elongation coefficient β is defined by:

$$\beta = \Delta / [n_b h_b (\theta - \theta_o)] \quad (1)$$

where Δ =beam elongation at a floor; θ =storey drift ratio; and θ_o threshold drift ratio, beyond which beam elongation occurs (0.5%). The physical interpretation of beta is that β multiplied by the beam height is approximately twice the distance between the neutral axis and the mid height of the beam; therefore, they suggest a value of approximately 2/3 for this coefficient.

Kim et al (2004) developed a joint model to represent the nonlinear behaviour of beam-column joint for reinforced concrete frame. The joint itself was assumed to behave rigidly and all inelastic actions were assumed to be at beam-column interface, the model was verified with experimental results of Zerbe and Durrani (1989) and the model captured clearly the beam elongation effect. Five storey, four-bay RC frame was analyzed with and without considering the beam elongation. Significant changes in the distribution of forces were observed considering the beam elongation effect; however this model did not consider slab effect.

Only a few have considered gap opening (beam relaxation) effects, which influence the frame/slab behaviour, such as Shahrooz et al (1992), the model was limited to the monolithic loading only. MacRae and Umarani (2006, 2007) have proposed a concept for considering slab effect on building seismic performance. They have developed simple model for explicit evaluation of the slab effect on moment-resisting structural systems which considers the slab contribution to the beam over strength. The model captures important aspects of the behaviour of reinforced concrete joint with a floor slab well. However, these studies were limited to single connections. Other very sophisticated models considering both effects were developed by Lau (2007); Peng (2009); Gardiner (2011). The models are very sophisticated, it requires large computational effort and time, accurate meshing and sufficient storage for the results. In despite the relative complexity of the model, there were some discrepancies between the analytical predictions and the experimental results.

The present paper initially analyses some test results, relevant to two subassemblies specimens tested under cyclic loads, to evaluate the effect of the slab and beam elongation. Successively, numerical simulations based on Finite Elements Models (FEMs) developed using the RUAUMOKO-2D have been performed to apply a simple model for a beam-column subassembly with a reasonable calibration for both the beam elongation/relaxation and the slab effects. The model developed should be capable of simulating pinching effect and stiffness degradation with expected hysteretic loop as in reinforced concrete structures; and finally, to examine the behaviour of a five-storey, four-bay reinforced concrete frame under dynamic loading conditions considering both slab effect and beam growth.

2 EXPERIMENTAL PROGRAM

2.1 Design of prototype frame

The prototype building was 27.6m long, 20m wide, five-storey high and four perimeter frames, spanning four bays in the longitudinal direction. The framing systems in the transverse direction were not considered in this study. The elevation view of the perimeter frame is given in Figure 1a. Each bay spanned 6.9m, and the storey height was 3.5m throughout the building. The typical lower interior subassembly, illustrated in Figure 1b, was considered for the experimental investigations. The prototype structure was designed for zones of high seismicity, Seismic Zone IV (PGA=0.5g) in accordance to the UBC (1997) assuming standard occupancy, type D-stiff, soil profiles. The effective

seismic mass at each floor was assumed to be 590t (1,300kips). The same size members were used over the frame height. Details of the material and member properties used in the frame analysis are summarized in Table 1. All the beams and columns were designed in such a way, that all yielding would occur only in the beams (satisfying the strong-column weak-beam concept), and satisfied most of the ACI-318 (2002) recommendations. The static pushover analysis, with inverse triangular lateral loads, was performed to identify the frame demand. The design storey drift was assumed to be 2% as per UBC (Section 1630.10) and the corresponding base shear was 2,000kN.

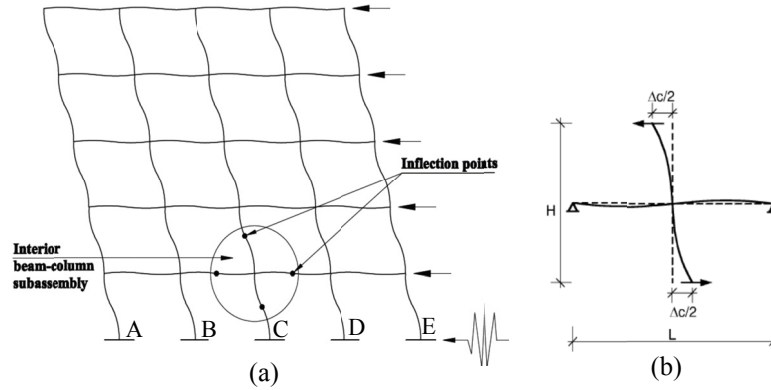


Figure 1. (a) Prototype frame subjected to seismic lateral loading (b) Modelling the interior beam-column subassembly

Table 1. Member properties for prototype frame

	Column	Beam	Slab
Size, $b_w \times h_b$ (mm×mm)	550×600	400×550	150 (thickness)
Compressive strength of concrete, f'_c (MPa)	35	35	35
Yield strength of steel, f_y (MPa)	414	414	414
Reinforcement	8-Ø25+4-Ø20	4-Ø25+2-Ø20 (top reinf.) 4-Ø20 (bottom reinf.)	Ø12@400mm c/c (straight) Ø12@400mm c/c (Bent)
Yield moment capacity (kN.m)	820	450	-

2.2 Test specimens

Two specimens represent approximately half-scale models were considered for the experimental test. Each specimen consisted of a column, two beams framing into the column on opposite sides, without transverse beams. The specimens had 275×300mm columns cross section and 275mm deep × 200mm wide beams. The geometry and reinforcement details of the test specimens are shown in Figure 2. The two specimens had the same size and reinforcement detailing for the beams, columns and beam-column joint. The first subassembly labeled “J” was constructed without a floor slab, while the second subassembly labeled “JS” had a slab, cast monolithically with the beam. The overall floor slab dimensions were 2.0m × 2.0m, with an average thickness of 63mm. The reinforcements of the slab were Ø6@250mm c/c in the parallel direction of the beam (longitudinal direction), and Ø8@200mm c/c in the transverse direction. Before the execution of the tests on the joint specimens, the mechanical properties of the constituent materials were determined and summarized in Tables 2 and 3.

The tests were carried out by applying the vertical displacements at the ends of the beams, as shown in Figure 3. The column was linked to a universal hinge connector at the bottom and to a box frame (with a swivel connector) at the top. The end of each beam was linked to the 250kN hydraulic actuator by a pinned-axial end. Thus the two ends of the beams and the top and bottom of the column were all pin-connected in the loading plane, to simulate inflection points of a frame structure subjected to lateral earthquake loading. The column pin-to-pin storey height (h_{co}) was 1.70m, and the beam pin-to-pin span length (L_b) was 2.2m. The pattern of cyclic displacements applied by the actuator during each test is given in Figure 3. A constant axial nominal compression load of 10% of the column axial capacity

was applied and kept constant throughout the entire test. More details on the test set-up and on the experimental program as a whole, can be found in (Ahmed and Umarani 2014).

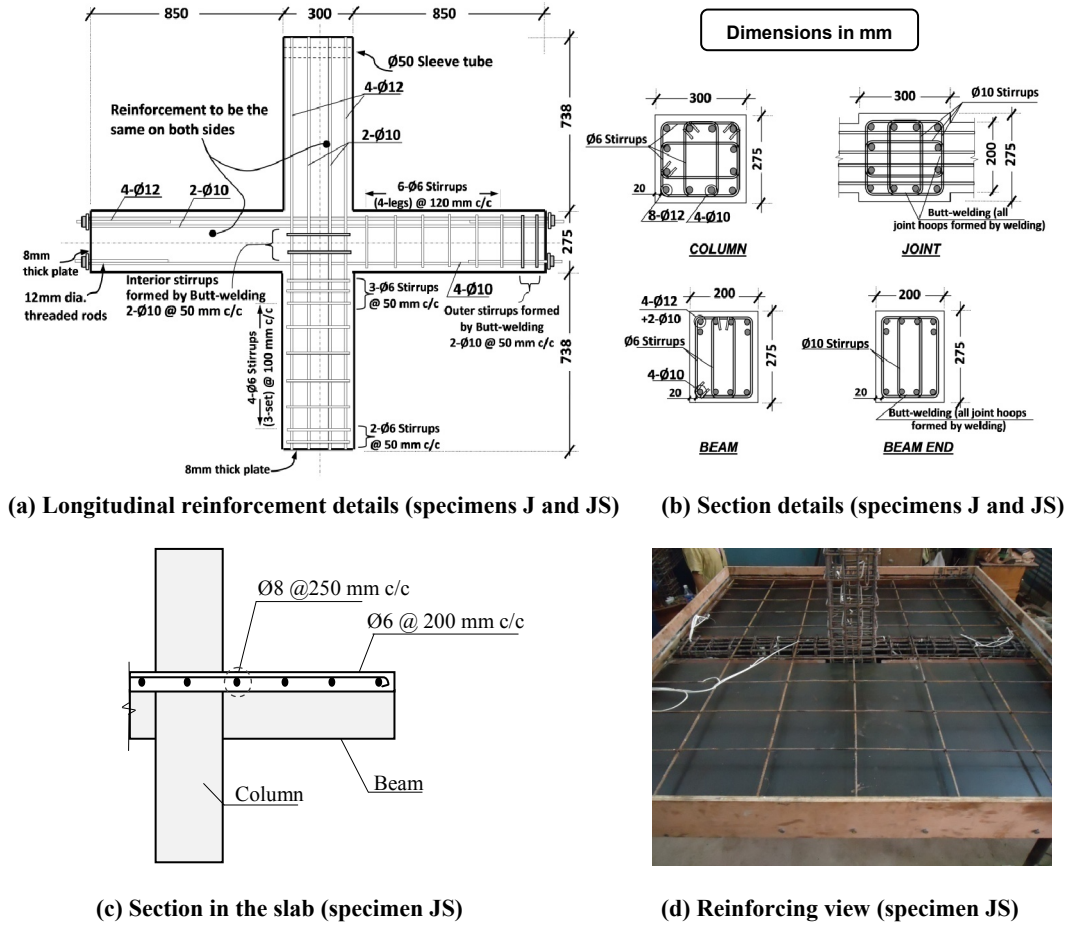


Figure 2. Reinforcement details of the specimens

Table 2. Reinforcement properties

Ave	Yield strength, f_y (MPa)	Yield strain, ϵ_y ($\mu\text{mm/mm}$)	Ultimate strength, f_u (MPa)	Elongation (%)
Ø6	469.3	2420	604.3	23.0
Ø8	459.0	2300	578.4	18.0
Ø10	451.1	2375	539.1	19.1
Ø12	477.2	2330	603.2	10.9

Table 3. Concrete strengths

Unit description	J	JS
28-days (MPa)	44.89	37.06
At testing day (MPa)	50.55	44.83

3 EXPERIMENTAL RESULTS

The two specimens performed in a ductile manner, with a plastic hinge forming at the beam end near the column face. There were only fine cracks in the column over the whole height, indicating that the column did not suffer major inelasticity. The desired strong-column weak-beam behaviour of the ductile frame was, therefore, achieved. No bond slip losses in the bars throughout the joint region, as in both specimens h_c/d_b ratio specified by ACI 352R (2002) (the ratio of the column depth to the largest bar diameter passing continuously through the joint) was 25, and greater than $20 \times f_y/420$ that provides longer development lengths and thereby minimizing the likelihood of the bar slips inside the joint region and prevent the extension of yielding to the column. This also will ensure stable hysteretic loops and less pinching effect with large energy dissipation capacity at a beam/column interface (within the plastic hinge region), as well as it provides a better observation for the beam elongation. As the main objective of the present paper is to identify the slab effect on the beam elongation, the experimental results of the two specimens relating to the beam elongation/ relaxation

are described below:

For both specimens, the elongation of the main beams was ineffective at a small drift levels below 1.5% (less than 1.5mm). Beyond this stage, the beams elongation was significantly increased due to extensive flexural cracks developed in the north and south beams near the face of the column (within the plastic hinge regions). Elongation of plastic hinges during large inelastic deformation occurs mainly from plastic strains in main reinforcement due to plastic rotation. Figure 4 shows the beam elongation for both specimens. However, the restraint in the beam elongation due to the floor slab were recorded nearly 14% at the 1.5% drift cycle, and become significantly higher (above 30%) at the larger drift levels. this restraint in the beam elongation due the presence of the floor slab was roughly near to equivalent 50% increase in the strength in the negative loading direction due to the tension floor slab. In other words the tension floor slab increased beam strength by average 60% and reduced the beam elongation by average 30% at large inelastic deformations (3.5% drift). The overall plastic hinges developed at beam/column interfaces at the end of the test are shown in Figure 5.

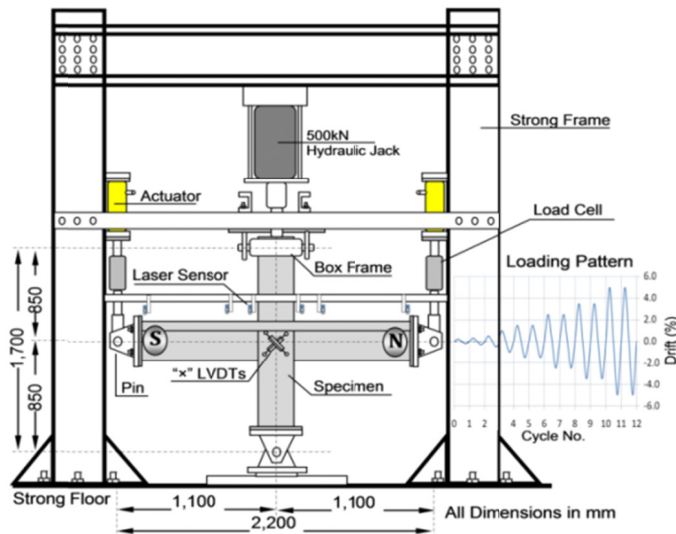


Figure 3. Test setup and Loading Pattern

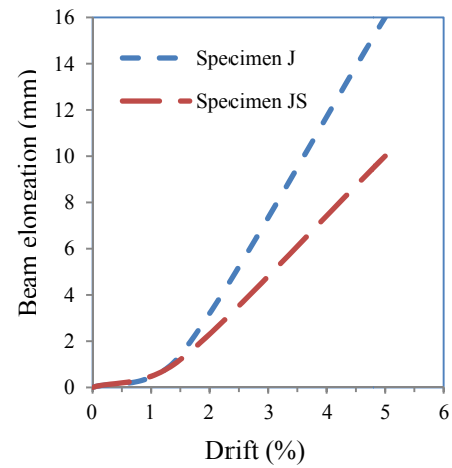


Figure 4. Beam elongation



(a) Specimen J



(b) Specimen JS

Figure 5. Final damage state at the north beam of specimens J and JS

4 ANALYTICAL MODELLING

The computational model shown in Figure 6 was used to simulate the beam-column joint region. A similar model had originally been developed to represent the gap opening and beam elongation behaviour at the beam-column joints, without considering the slab effect in reinforced concrete frame and precast systems, Kim et al (2004). Subsequently, MacRae and Umarani (2006, 2007) improved this model by introducing the slab effects. The model was modified and used in this study. The model was constructed in RUAUMOKO-2D and it uses elements from the standard library.

In this model, the strong column and strong panel zone are assumed such that all inelastic deformations occur in the plastic hinge region near the ends of the beams. Moments are transferred between the beam and column by horizontal tension and compression components between node pairs.

Two parallel sets of elements connect the nodes in each pair. One is an inelastic truss element that simulates the mild steel and resists tension or compression. The other is a multi-spring element which has inelastic properties in compression but has no tension strength and it represents the cracked concrete. The beams and columns were modelled as elastic members with cracked sectional properties using 4-noded frame elements. In the current study, a value of 40% of I_{gb} was used to model the beam elements (Paulay and Priestley 1992). Similarly, the effective moment of inertia of the column, I_{ec} , is assumed to be in a range of 40% to 80% of the gross moment of inertia, I_{gc} , depending on the level of axial load (Paulay and Priestley 1992). A simple equation is used to estimate the effective moment of inertia, for cracked concrete columns as proposed by Nuncio and Priestley (1991):

$$\frac{I_{ec}}{I_{gc}} = 0.21 + 12 \rho_l + \left[0.1 + 205 (0.05 - \rho_l)^2 \right] \times \frac{P_{axial}}{A_g f'_c} \quad (2)$$

where, ρ_l is the total longitudinal reinforcement ratio of the column, P_{axial} is the axial load on the column, f'_c is the concrete compressive strength, and A_g is the column gross area.

The truss element for the reinforcing steel with Clough degradation hysteresis (1981) was selected to provide the appropriate force-displacement characteristics. The strain-hardening ratio of the steel was assumed to be 0.02. The stiffness property of mild steel was calculated, based on the length of yield which is assumed as the sum of the depth of the beam, plus twice anchorage length. The properties of the concrete gap elements were assigned based on the plastic hinge length (Priestley et al 1996) and an elasto-perfectly plastic stress-strain curve with a yield strain of 0.003 at the compressive strength f'_c .

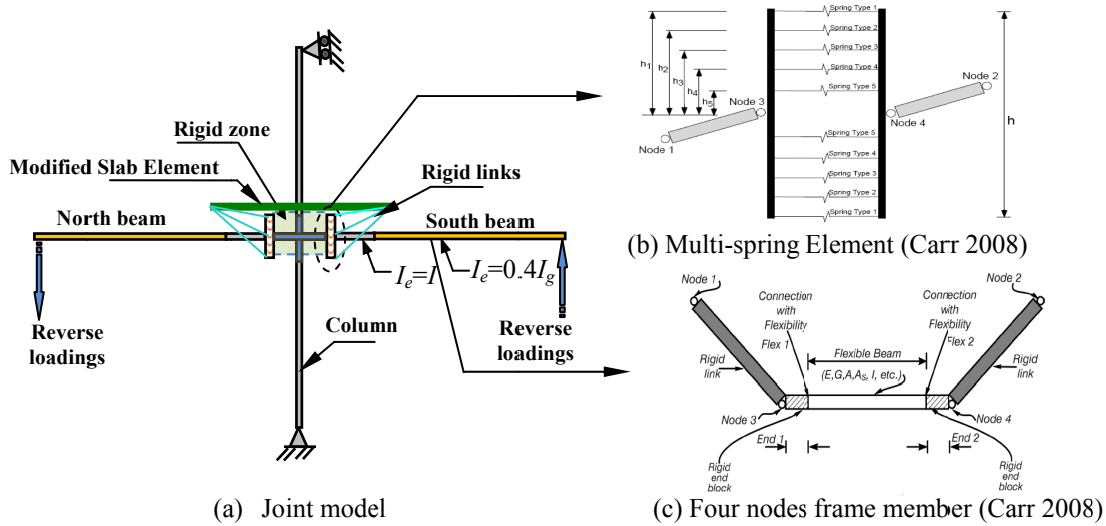


Figure 6. Computation model in RUAUMOKO for slab-beam-column joint

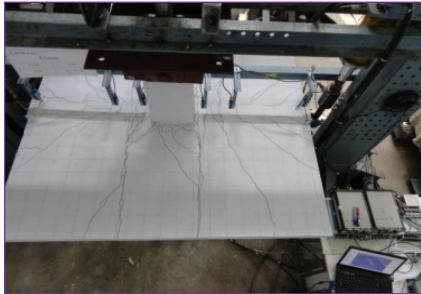


Figure 7. Crack pattern in the slab of specimen JS

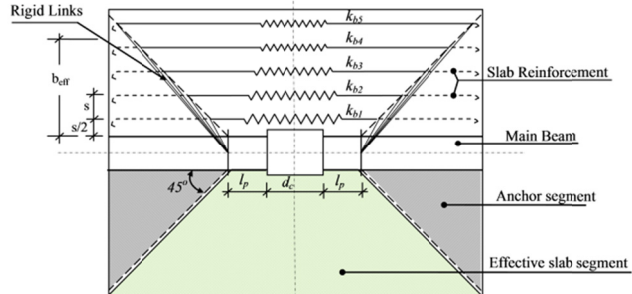


Figure 8. Slab modelling

In the current experimental test and previous literatures (Cheung et al 1987; Pantazopoulou et al 1988; French and Moehle 1991), large tensile strains develop in the reinforcement across the slab near the longitudinal beam, and decrease with increasing distance from the beam. Hence the cracks in the slab at the beam-column subassembly were observed to start from the length equal to the effective beam depth (plastic hinge length, l_p) from the column face and extended at approximately a 45° angle, as

shown in Figure 7. Thus, in the current model, the effective slab segment between the yield lines where cracking is expected, as shown in Figure 8.

The effective steel in the slab (effective slab segment) is assumed to be anchored outside this zone. The stiffness property of slab reinforcing steel, ($k_{bi}=EA_b/L_s^i$) is calculated, based on the length of yield of each bar within effective width. The effective slab width in tension (b_{eff}) shown in Figure 8 are calculated as effective of main beam width plus two times the beam height from each side of main beam (Pantazopoulou et al 1988, Zerbe and Durrani 1990).

5 RESULTS OF ANALYTICAL VERIFICATION

The model was used to evaluate the cyclic behaviour of beam-column subassemblies with and without floor slab that were tested in the current study. The element properties were directly related to the physical properties of the system. Figure 9 shows the comparison of the model results with the experiment results. A satisfactory agreement between the analytical and experimental results is observed. The hysteretic curves drawn to the same scale are the most significant results. Since the measured and predicted values were similar during cyclic loading, the slab effect at the subassemblies appeared to be significant.

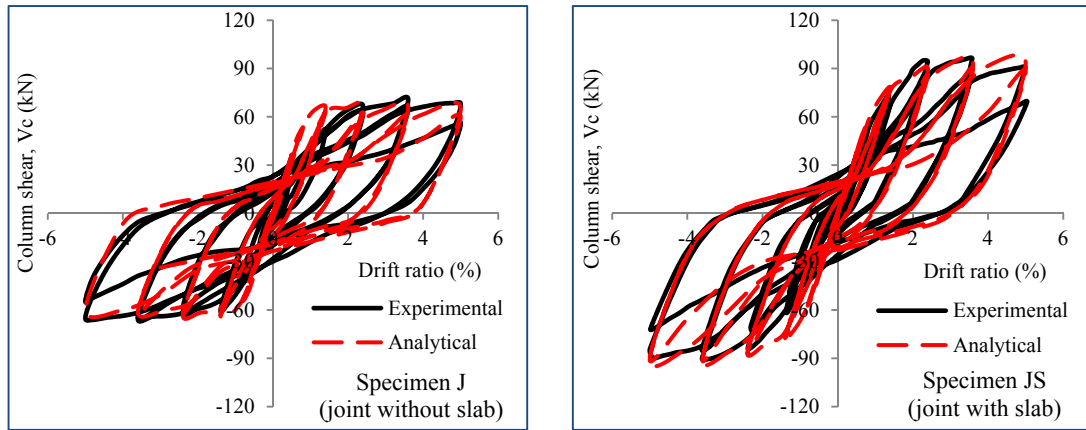


Figure 9. Validation of model with test results

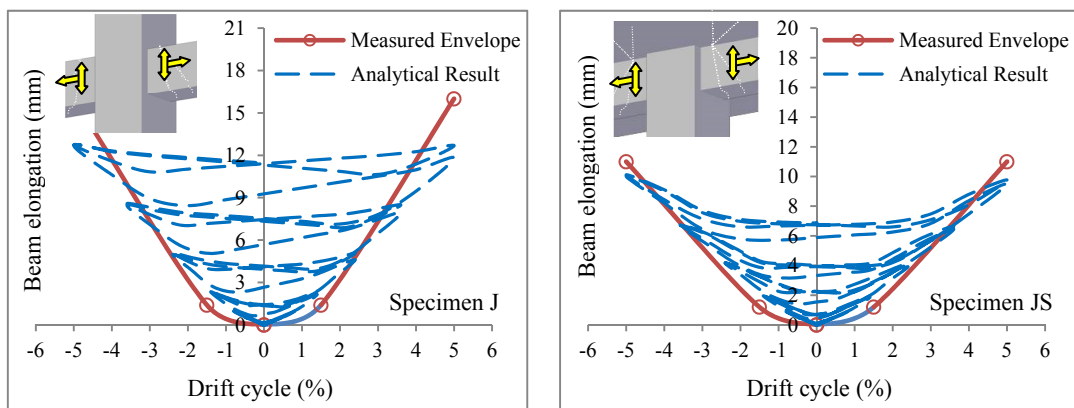


Figure 10. Beam elongation/relaxation vs. drift ratio for both specimens

The pinching effects shown in the global behaviour are essentially caused by both yielding of the reinforcements and concrete cracking at the plastic hinge regions. Both the models, including and excluding the slab effect can account for the influence of the beam elongations with reasonable precision (Figure 10). It can be noted that, the beam elongation increases as the flexural inelastic deformation increases. However, during repetition of the same cycle, with no increase in the flexural

deformation, member elongation continues to increase. Also the floor slab can significantly reduce this elongations, especially at a large deformation levels (drift ratios $>1.5\%$). This effect can be further investigated in the analysis of the multi-connections frame; however, the elongation of the main beams is partially restrained by the exterior columns, which results in axial compression in the main beams.

6 BEHAVIOUR OF PROTOTYPE FRAME UNDER SEISMIC LOADING

To complement the experimental and analytical investigation on the seismic performance of the connections, a series of inelastic dynamic analyses were performed on the prototype frame under selected earthquakes to study the influence of the floor slab on the overall behaviour of the prototype frame. The classical Newmark integration method was used ($\gamma=1/2$, $\beta=1/4$), with a time step of $\Delta t=0.01s$ and a total of 2000 steps (input time: 20sec.) for integrating the produced equation of motion. The distribution of mass in the model was using the lumped mass approach. The damping coefficients were chosen such that the viscous damping for the entire structure was 5% (Chopra 2000). Two ground motion records, representing different characteristics and intensity were chosen for the dynamic analyses: The El-Centro (1940) records ($PAG=0.348g$) were selected to represent far field ground motions while the Northridge (1994) records ($PAG=1.284g$) were selected because of their near-fault characteristics. Two analytical models were developed to represent the behaviour of an indeterminate reinforced concrete frame. The RFIS model included the slab effects, while the other model (RFES) was based on excluding this effect. By comparing the RFIS and RFES model responses, the effects of the floor slab could be examined.

6.1 Global responses

The results of the typical base shear response for the RFIS and RFES models under Northridge earthquake are plotted in Figure 11. The floor slab at the frame joints appeared to be significant; the maximum base shear of the RFIS model was 28% higher than the model based on excluding this effect (RFES model). The floor slab effect on the individual response characteristics are discussed below:

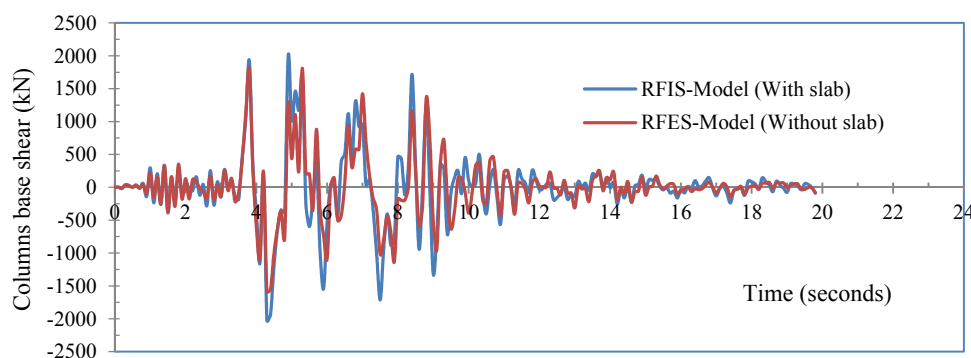


Figure 11. Column base shear response for the prototype frame under Northridge earthquake (1995)

- i) Columns response: The distribution of maximum storey shear demand from the two seismic events is shown in Figure 12 for the RFIS and RFES models. Under El-Centro earthquake the ratios of the base columns shear of the RFIS model to that of the RFES model were 1.09 and 1.03 in positive and negative loading directions, respectively. A tension floor slab effect had a larger participation under larger seismic events when the yielding started to occur and the beams started to grow in its length. Under the Northridge earthquake, the ratios of the base columns shear of the RFIS model to that of the RFES model were 1.10 and 1.28 in positive and negative loading directions, respectively. This was reasonable, since the RFIS model had a higher stiffness value compared to the RFES model, especially after beam elongation started to occur. However, a larger base shear forces will be expected due to the presence of the slab with larger drift deformation levels.

- ii) Column moments demands: The maximum column moments at the first storey for the RFIS and RFES models are compared in Figure 13. The bending moments in the ground storey columns is increased in an average of 5% and 12% due to the tension slab, corresponding to El-Centro, and Northridge earthquakes respectively. These increases were due to the floor slabs restraining the gap opening at the first floor level and thereby inducing beam axial forces. These forces increased the bending moments by the fact that the column bases are fixed to an inextensible foundation.

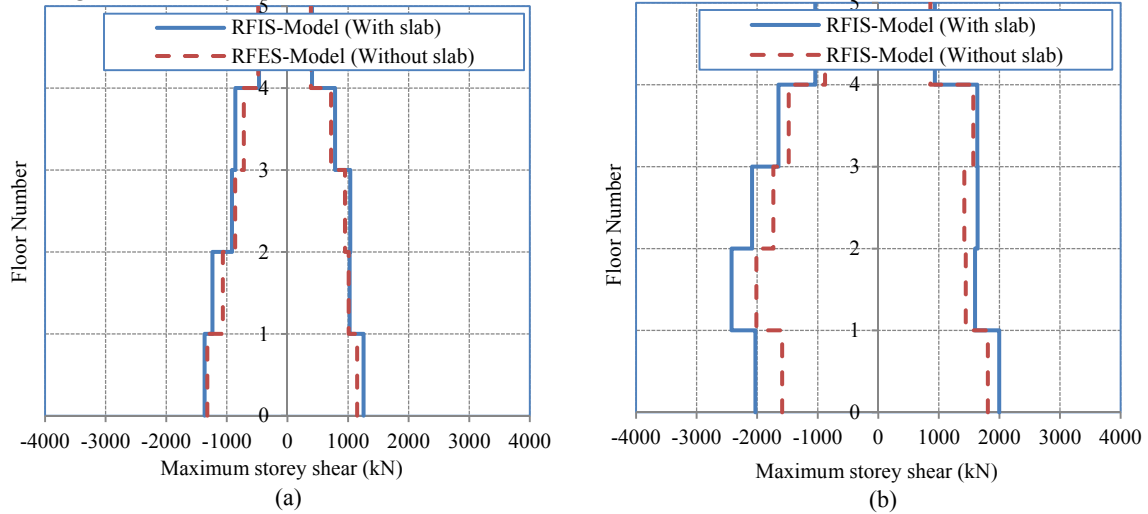


Figure 12 Distribution of maximum storey shear under (a) El-Centro and (b) Northridge earthquakes

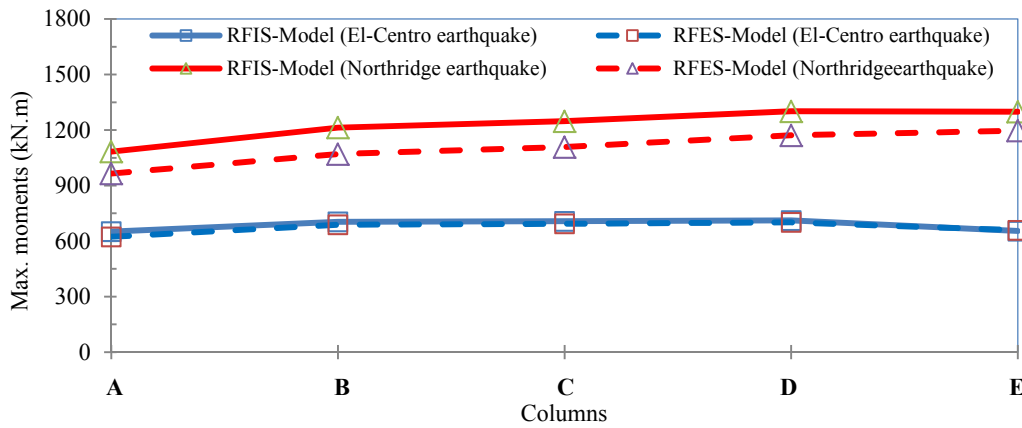


Figure 13. Distribution of column moments at first storey

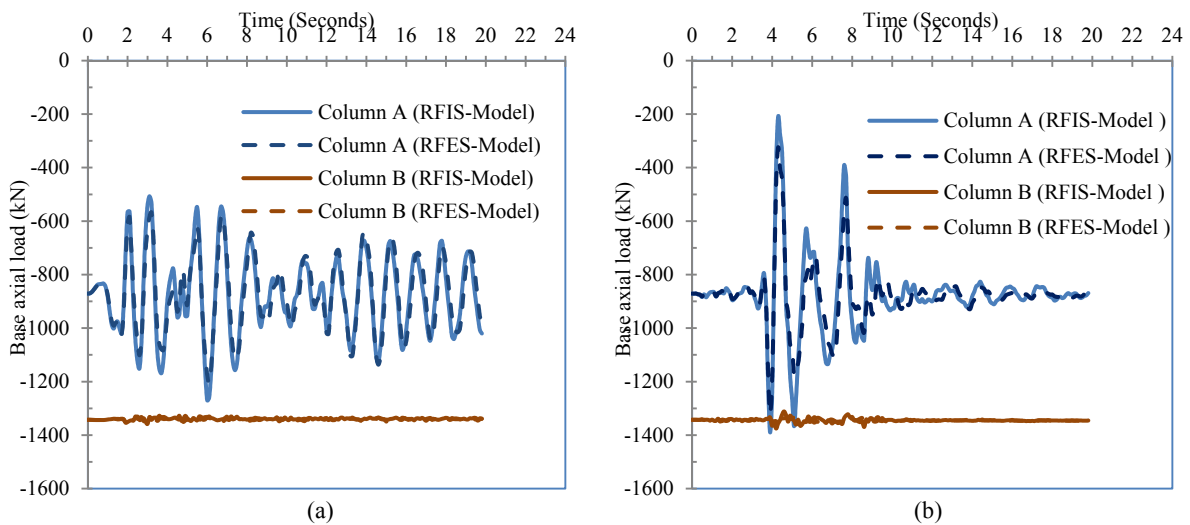


Figure 14. Base axial fluctuation of outermost column (Column A) and the column near central column (Column B) under (a) El-Centro and (b) Northridge earthquakes

- iii) Column axial load fluctuation: A large amount of axial load fluctuation was observed for the outermost column (columns A and E), as shown in Figure 14. The responses did not produce tensile force on the outermost column with an intense seismic excitation, but it was close to that, especially under Northridge Earthquake when the slab effect was considered. In general, both earthquake excitations produced less significant fluctuation for the other columns (columns B, C and D) compared with the outermost column.

6.2 Effects of beam elongation/relaxation

The hysteretic curves of the total beam elongation at each floor level for the RFIS and RFES models under the two ground motions (Figures 15 and 16), demonstrated that the beam elongation occurs at all floors of the frame. It is significantly larger in the floors with higher levels of drift ratio. It is clearly shown, the beam elongations were insignificant at drift ratios lower than 1.5% (El-Centro earthquake); as the inter-storey drift angle exceeded 1.5% (approximately the limit of the yielding) the beam elongations increased significantly, especially under strong ground motion (drift angle >3.0%).

The maximum beam elongation values were at the second storey, and become significantly larger at a strong ground motions. Since the beam elongation occurs particularly at the column interface, while the slab is intact, it restricts the gap opening at the beam ends, and changes significantly the beam elongation across the building. In these figures, the estimated beam elongation at each floor level which represented by a horizontal dash line, is calculated based on Eq. (1) (by substituting the beam depth h_b , number of bays n_b , threshold drift ratio of 0.5% and the corresponding maximum drift ratio θ at each floor level). This equation cannot be used for the drift ratios less than 0.5%, therefore some floors did not contains this limit (Figure 15a and e). However, this limit looks under-estimated for the first floor and over-estimated for the roof. Generally, it provides a reasonable estimation for the beam elongation.

7 CONCLUSIONS

As seen in the preceding discussion, ignoring the slab effect is possible to significantly underestimate the strength of a structure and the failure mechanism of the structure might be different from the one anticipated. The structure may also experience unexpectedly high elongation at all floor levels, if the floor slab contribution is not considered properly. The major findings of this study are as follows:

- The current experimental investigation demonstrated that the elongation of the main beams was ineffective at a small drift level below 1.5%. Beyond this stage, the beam elongation was significantly increased due to extensive flexural cracks developed within the plastic hinge regions. However, during repetition of the same cycle, with no increase in the flexural deformation, member elongation continues to increase and the floor slab can significantly reduce this phenomenon, especially at a large deformation levels (drift ratio >1.5%).
- The developed joint model predicts the test results with reasonable precision, and provides a simple way of accounting for the effects of slab and beam elongation, without a complicated nonlinear Finite Element modeling. However, to accurately evaluate the subassembly behaviour for substandard frame building joints (joints non-codal designed), the cases with bond-slip loss within the joint should be considered.
- The multi-storey frame analytical results demonstrated that the beam elongation occurs at all floors of the frame. It was significantly larger in the floors with higher levels of drift ratio. The floor slabs restrain this phenomenon and cause the columns to displace by different amounts and increasing the base shear of the columns. The effect of floor slab including beam elongation effect is thus illustrated for a two dimensional moment frame building and this model works well for the lateral load analysis of frames.

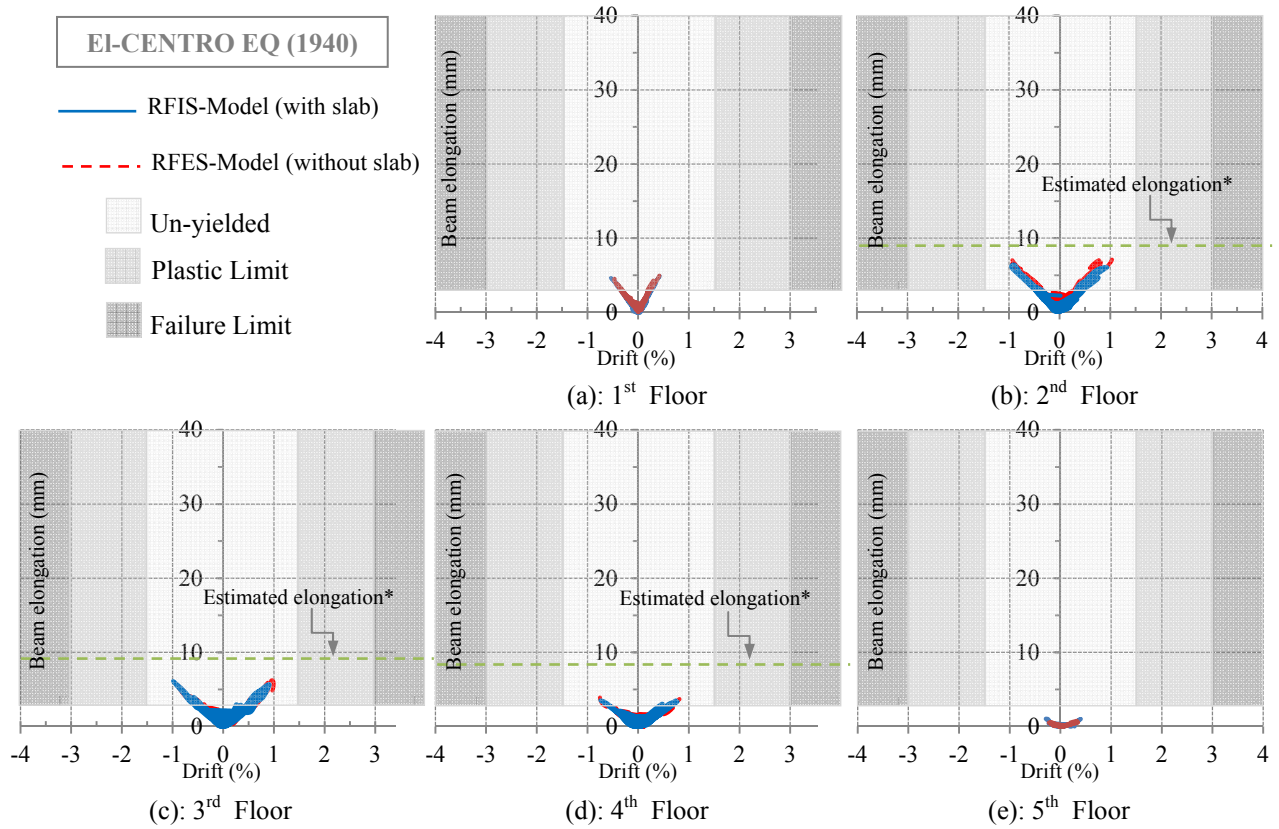


Figure 15. Beam elongation vs. central column drift ratio under EI-Centro earthquake

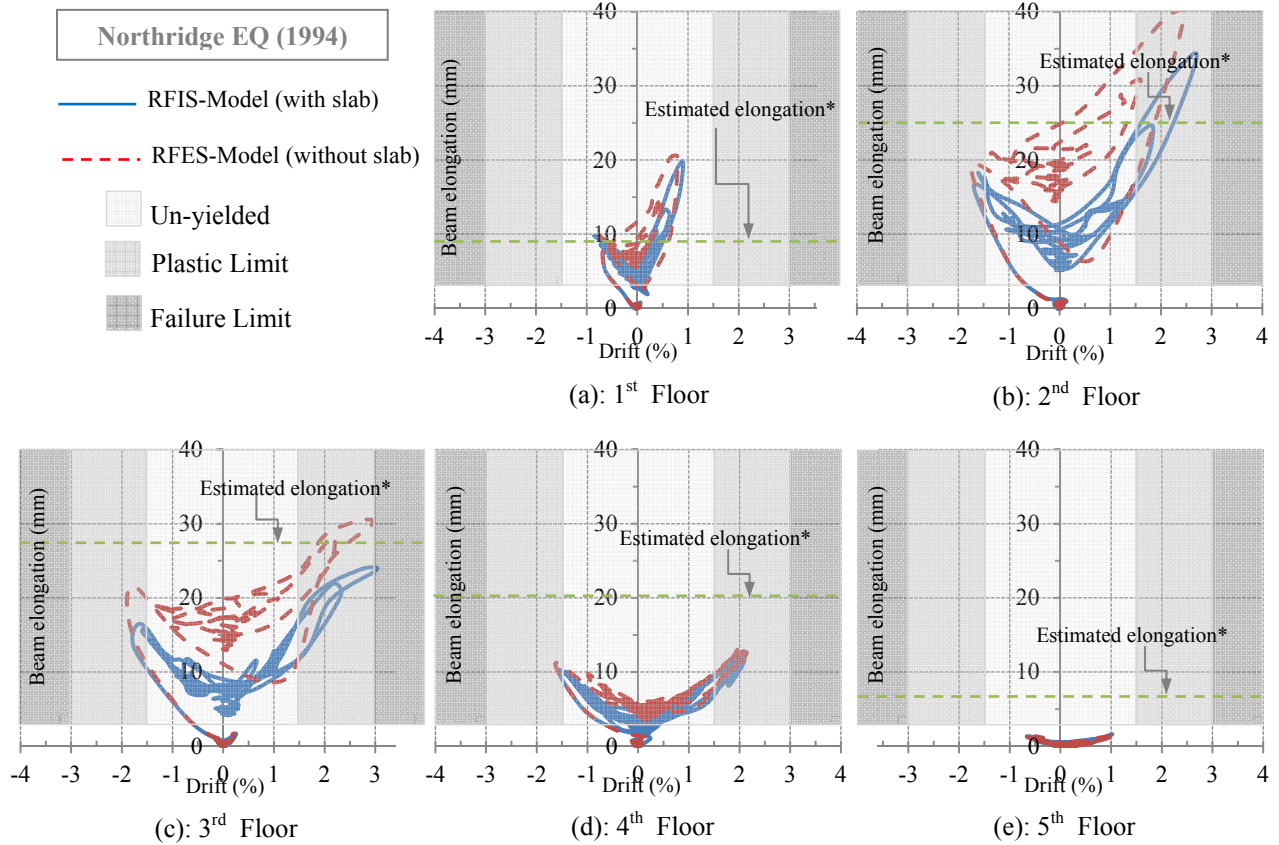


Figure 16. Beam elongation vs. central column drift ratio under Northridge earthquake

REFERENCES

- ACI Committee 318 2002, Building code requirements for reinforced concrete, *American Concrete Institute*, Detroit.
- Ahmed, S.M. & Umarani, C. 2014, 'Testing and evaluation of reinforced concrete beam-column-slab joint', *Journal of the Croatian Association of Civil Engineers (GRADEVINAR)*, Vol. 66, Issue 1, pp. 51-66.
- Calvi, G.M. Magenes, G. & Pampanin, S. 2002 'Relevance of beam-column joint damage and collapse in rc frame assessment', *Journal of Earthquake Engineering*, Special Issue, Vol 16(2), 75-100.
- Carr, A.J. 2008 'RUAUMOKO 2D': User manual, computer program library, Department of Civil Engineering, University of Canterbury, Christchurch, New Zealand.
- Cheung P., Paulay, T. & Park. R. 1987, A reinforced concrete beam column joint of a prototype one-way frame with floor slab designed for earthquake resistance, Research Report, 87-6, University of Canterbury, NZ.
- Chopra, A. K. 2000, Dynamics of Structures, Pearson Education, USA.
- Durrani, A. J. & Zerbe, E.Z. 1989 'Seismic response of connections in two-bay R/C frame subassemblies', *Journal of Structural Engineering, ASCE*, Vol 115(11), 2829-2844.
- Cheung P., Paulay, T. & Park. R. 1987, A reinforced concrete beam column joint of a prototype one-way frame with floor slab designed for earthquake resistance, Research Report, 87-6, University of Canterbury, New Zealand.
- Ehsani, M.R. & Wight, J.K. 1985 'Effect of transverse beams and slab on behavior of reinforced concrete beam-to-column joints', *American Concrete Institute ACI*, Vol 82(2), 188-195.
- Eligehausen, R., Özbolt, J., Genesio, G., Hoehler, M. S., & Pampanin, S. 2006 '3D modelling of poorly detailed RC frame joints', NZSEE conference, Paper No. 23.
- Elmorsi, M., Kianoush, R.M., & Tso, W.K. 2000 'Modelling bond-slip deformations in reinforced concrete beam-column joints', *Canadian Journal of Civil Engineering* Vol 27 (3), 490-505.
- Fabbrocino, G., Verderame, G. M., Manfredi, G. & Edoardo, C. 2004 'Structural models of critical regions in old-type RC frames with smooth rebars', *Engineering Structures*, Vol 26(4), 2137-2148.
- Favvata, M., Izzuddin, B. & Karayannis, C. 2008 'Modeling exterior beam-column joints for seismic analysis of RC frame structures', *Earthquake Engineering and Structural Dynamics*, Vol 37(13), 1527-1548.
- Fenwick, R. & Davidson, B. 1995 'Elongation in ductile seismic resistant reinforced concrete frames', *American Concrete Institute, ACI*, Special Issue, Vol 157(7), 143-170.
- Fenwick, R. & Fong, A. 1979, The behaviour of reinforced concrete beams under cyclic loading, Research Report, 176, University of Auckland, Auckland, New Zealand.
- Filippou, F.C., Popov, E.P. & Bertero V.V. 1983, Effect of bond deterioration on hysteretic behavior of reinforced concrete joints, EERC Report 83-19, Earthquake Engineering Research Center, University of California, Berkeley, California.
- French, C.W. & Moehle, J.P. 1991 'Effect of floor slab on behaviour of slab-beam-column connections, design of beam-column joints for seismic resistance', *American Concrete Institute*, Special Issue, 123, 225-258.
- Gardiner, D. 2011, Design recommendations and methods for reinforced concrete floor diaphragms subjected to seismic forces, Ph.D thesis, University of Canterbury, Christchurch, New Zealand.
- Kim, J., Stanton, J. and MacRae G.A. 2004 'Effect of beam growth on reinforced concrete frames', *Journal of Structural Engineering, ASCE*, Vol 130(9), 1333-1342.
- Lau, D. & Fenwick, R. 2002, 'The influence of precast prestressed flooring components on the seismic performance of reinforced concrete perimeter frames', *SESOJ Journal*, Vol 14(2), 17-26.
- MacRae, G.A. & Umarani, C. 2006 'A concept for consideration of slab effects on building seismic performance', NZSEE conference, Paper No.22.
- Nuncio, C.A. & Priestley, M. 1991, Moment overstrength of circular and square bridge columns, Technical Report Report No. SSRP -91/04, Department of Applied Mechanics and Engineering Sciences, University of California, San Diego.
- Otani, S. 1981 'Hysteresis models of the reinforced concrete for earthquake response analysis', *Journal of Faculty of Engineering*, Vol 36(2), 407-441.
- Pantazopoulou, S.J., Moehle, J., Shahrooz, B.M. 1988 'Simple analytical model for T beams in flexure', *Journal of Structural Engineering*, Vol 114(7), 1507-1523.
- Paulay, T. & Priestley, M. 1992, Seismic design of reinforced concrete and masonry buildings, John Wiley and Sons, Inc.
- Peng, B.H.H. 2009, Seismic performance assessment of reinforced concrete buildings with precast concrete floor systems, Ph.D thesis, University of Canterbury, Christchurch, New Zealand.

- Priestley, M., Seible, F. & Calvi, M. 1996, Seismic design and retrofit of bridges, Wiley, New York.
- Shahrooz1, B.M., Pantazopoulou, S.J. & Chern, S.P. 1992 'Modelling slab contribution in frame connections', *Journal of Structural Engineering, ASCE*, Vol 118(9), 2475-2494.
- UBC 1997, Handbook to the Uniform Building Code, An Illustrative Commentary. Whittier, California: International Conference of Building Officials.
- Umarani, C, & MacRae, G.A. 2007 'A new concept for consideration of slab effects on building seismic performance', *Journal of Structural Engineering SERC*, Vol 34(1), 25-32.
- Unal, M. & Burak, B. 2013 'Development and analytical verification of an inelastic reinforced concrete joint model', *Engineering Structures*, Vol 52, 284–294.
- Zerbe, H.E, Durrani, A.J. 1990 'Seismic response of joints in two-bay reinforced concrete frame subassemblies with a floor slab', *American Concrete Institute, ACI*, Vol 87(4),406-415.